Indian Journal of Chemical Technology
Vol. 31, November 2024, pp. 840-850
DOI: 10.56042/ijct.v31i6.11879

Comparative study of machine learning models for removal of As(III) from potable water using spiral-wound nanofiltration and analyzing input responses

Deepak Koundal, Mohit Sehgal & Shailendra Bajpai*

Department of Chemical Engineering, Dr. B R Ambedkar National Institute of Technology, Jalandhar-144 008, Punjab, India

*E-mail: bajpais@nitj.ac.in

Received 18 June 2024; accepted 3 October 2024

An attention toward health disorder and numerous health illnesses is the root cause of increase in heavy metal contaminants such as Arsenic(III) in potable water. An effective remedy for this problem is a nano-filtration membrane, which is affordable and doesn't allow heavy metal ions to permeate. However, for better outcomes input parameters should be gauged at an accurate value, which is quite challenging. This study addresses the complexity of employing artificial neural network (ANN) to model the percentage rejection of a nano-filtration membrane using deep learning toolbox in MATLAB. Three different algorithms, i.e., Levenberg-Marquardt, Bayesian regulation, and scaled conjugate gradient, have been used for training, and the best results are shown by Bayesian regulation algorithms and hence selected for this study. The number of neurons in the hidden layer is specified as 10, which provides the mean square error ($4.7 * 10^{-7}$) and coefficient of correlation (1), which signifies a well-trained model. Following an examination of trained model by verification and validation then the various input responses response was studied. The optimum percentage rejection of As(III) removal occurred when feed concentration, transmembrane pressure, and feed flow rate were between 30 to 50 mg/L, 5.71 to 7.09 bar, and 12.5 to 17 L/min, respectively, when temperature and pH are under the nominal range, i.e., 303K and 8, respectively.

Keywords: Artificial Neural Network, Arsenic removal, Deep learning, MATLAB, Mean square error, Nano-filtration

Introduction

Heavy metal, particularly Arsenic (As), is toxic in nature and is found majorly in sources like groundwater. Perhaps after the industrialization, an major anthropogenic activity, contamination of As(III) in drinking water have crossed the Bureau of Indian Standards (BIS) limits, i.e., less than 10 parts per million[1]. The metal is available as arsenates and arsenides in plant earth crust in abundant. Arsenite [As(III)] and Arsenate [As(V)] are to two major forms in which it exists in water. However, if the water is oxygenated As(III) converts into As(V). As(III) is far more hazardous than As(V) in water. Data presented by the World Health Organization (WHO), (2022) estimated that around at least 140 million people living in 70 countries globally who are exposed to drinking water containing As(III) breaching the prescribed permissible limits[2]. Being extremely toxic, As(III) cause fatal disease like cancer and body disorder if its concentration is lower and consumption for long duration. However, if concentration is high it will cause deadly mishap like death[3].

High concentrations of As in water are found mainly in Asian countries such as Bangladesh, India, Vietnam, and Myanmar[4]. Removal of such toxic contaminates is must and becoming essential as a result of demand of public awareness provided by health department. Researchers have developed a number of solutions, such as adsorption[6], electrochemical precipitation[7,8], liquid-liquid extraction[9], membrane separation[10,11], and ion exchange[12]. Still, the pressure-driven membrane (PDM) separation process finds the most predominant solution for removing heavy metals[13].

The PDM is a membrane filtration technique that uses the principle based upon the difference in particle and pore sizes to separate a mixture of liquid-liquid or liquid-solid. However, applied pressure works as the driving force of operation. The classification of PDM is divided into four categories: RO (reverse osmosis), NF (nanofiltration), MF (microfiltration), and UF (ultra-filtration)[14]. Since NF only permits monovalent ions to enter the permeate stream, NF is consider for this study. Recent research by Fang *et al.*[15] shows that, when operating at nominal pH (6–8), As(III) can be extracted from water using NF and is under the intended permeate limit.

Criscuoli *et al.*[16] reported the fabrication of an polyamide NF (effective surface area of 500 cm^2) spiral wound membrane and its use it in a pilot plant for the removal of As (III). The output was less than 10% As in the permeate stream when the concentration of feed is set in the range of 0.02–0.06 mg/L. In the permeate stream, they specifically get less As (III) than As(V). The effective rejection of As(III) was found to be 86%–96% higher than As(V) as observed by Nguyen *et al.*[10] when thin film polyamide composite NF membrane was used and experiment was conducted as a plate and frame module with an effective surface area of 79 cm^2 and operated in the nominal pH range (6–8). The rejection efficiency of As(III) was 86%–96%, as compared to 41-44% of As(V).

The three dimensional plot of a NF is shown in Fig. 1, where particles with larger sizes cannot permeate through membrane pores, particles smaller than membrane pores can easily permeate and enter the permeate stream. There are various PDM flow setups for membrane separation. Cylindrical tube, plate and frame, hollow fibre, and spiral wrapped are the four forms that are most frequently utilized in home and commercial applications. However, when comparing the benefits of each of these configurations, it is found that the spiral wound configuration is the best among others because it has a greater flux and a better surface area due to a better packing density. Ribera *et al.*[17] has compared with other membrane configurations and found that the spiral wound membrane is more effective. As, Cd, Cu, and other heavy metals can be eliminated by the NF membrane as it functions between UF and RO[18, 19].

Although NF appears to be a promising solution in terms of efficiency, availability, and handling operation compared to other modules, attaining a good percentage rejection (% rejection) is at most priority that cannot be eliminated, which makes it a limitation for the usage of NF at commercial scale. A good percentage rejection depends mostly upon operating parameters such as transmembrane pressure (TMP), feed concentration, pH, time of operation, input flow rate etc. working under severe conditions leads to a decrease in efficiency, ultimately affecting % rejection[20].

To have an optimum working range, extensive experimental work is to be performed, and the result will be obtained, but that will consume many resources, and to substitute that simulation make a pivotable role. Mathematical models are necessary for the simulation and optimization of the process. In the present decade, with the introduction of 3 generation of www and the development of Artificial Intelligence (AI) and Machine Learning (ML), several new techniques, including Artificial Neural Network (ANN), Fuzzy Logic, Genetic Programming, and Supported Vector Machines, have been introduced. ANN is the most promising and popular ML tool because it behaves similarly to a human brain[21]. It also has nodes connected to each other, similar to the human brain. These nodes create a relation from the given responses and target variables. ANN also have a

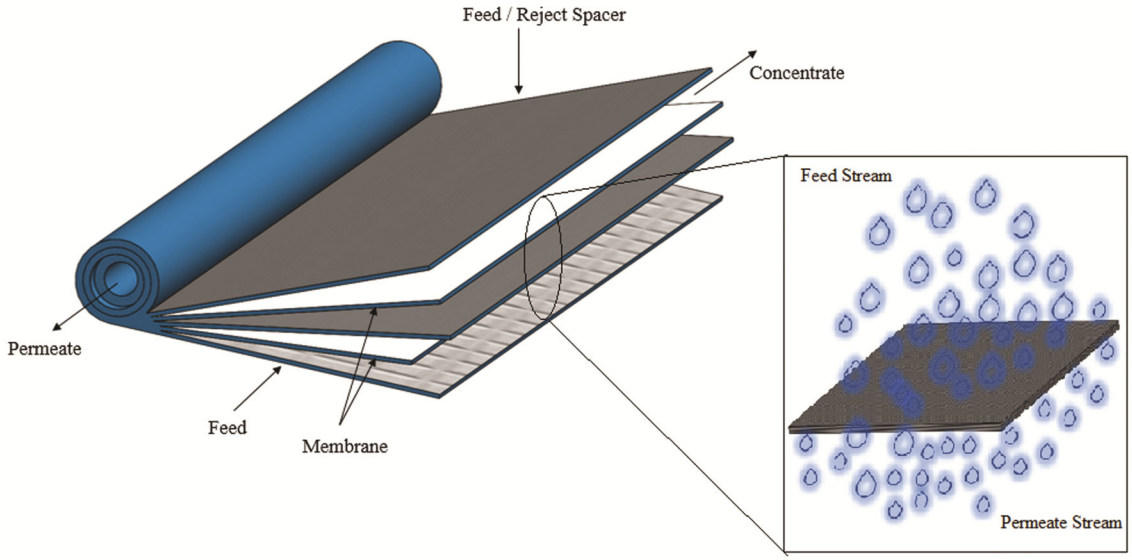

Fig. 1 — Schematic diagram of PD crossflow NF

leading edge compared to other conventional modes as it can work easily with non-linear functions, noisy data, incomplete data, have the capability to handle multiple input and multiple output problems(MIMO) , provide high accuracy, and take less computational time[22].

Through the development of an ANN, Bowen *et al.* predicted that salt would be rejected from a mixture through the NF process. In addition to maximising the operating parameters, scientists take into account each ion's diffusion and feed concentration[23]. The total dissolved solids were predicted by Zhao *et al.*[24] utilising solution diffusion passing from an NF from the Spiegler–Kedem model. An all-encompassing municipal water filtering solution was obtained by using the ANN model developed in the Shetty *et al.* to study to a series of NF experiments. It was then possible to forecast the permeate concentration to feed concentration ratio using the created model[25]. Darwish *et al.* used ANN model to compute rejection by providing an input of three different NF membranes ranging from pressure and permeate flux. They used the regularization-training algorithm because it performs better than other comparative algorithms. The results show a good prediction value and took less computational time[26]. Walter *et al.* used AI and ML and ANN modelling for timely and efficient heavy metal pollutant removal for wastewater treatment. The trained model predicted a solution with the optimal conditions of pH 3, operation time of 60 min and COD of 1.5 mg/L. Yao *et al.* used ANN modelling for removal of SO_4^{2-} which is influenced by various parameter. As a result multilayer perceptron predicted a superior sulfate removal compared to radial biases function network. Alardhi *et al.* conducted a comparative study on Reverse Osmosis Experiment from RSM and ANN, where ANN model showed a better prediction as the Performance error was less than 0.0003 and coefficient of relation was 0.9999 and RSM Coefficient of relation is restricted to 0.988. This shows the wide use of ANN, which is not confined to membrane parameters, but it extends to several other science domains such as polymer synthesis and desalination and many more[27].

According to several Health NGO's, United States and China, India has most heavy metal contaminated drinking water which will affect the human resource and not suitable for country growth. So, an urgent remedy is required. PDM are very effective, efficient, affordable solution and accessible in remote location. However, the working parameters should be gauges in optimum range. To find these optimum working range, large time and knowledge is required.

Along with that non availability of sufficient data is a challenge for modelling. Hence machine learning model will help to find the optimum parametric range, attaining a good membrane life as well as quality of outlet water. However, not many publications have been published related to the optimized study of the heavy metal rejection from NF using modelling and simulation software. Perhaps this make an conclusion that modelling and simulation for NF is a green field and a lot work is to be done which will be helping society in terms of monetary, technical benefits.

In this study, an ANN model is developed using 3 different algorithms that are trained, tested, and validated. Among the best algorithms, results are selected for modelling and simulation. ANN is provided with input responses that are: TMP, Concentration of Feed, Temperature, pH, Feed Flowrate and Operation Time where the predicted value is %Rejection. We studied the effect of these parameters on the output. The experimental details are taken from previous results[28].

Experimental Section

Prior to the advancement of computational methods, researchers employed traditional design of experiment (DOE) procedures to establish relationships between input responses and output parameters. Factorial design and Response Surface Methodology are some of wide spread examples of DOE. Response Surface Methodology (RSM) modelling is used in a study done by Gasemloo *et al.* to enhance the effective removal of Cr(VI) ions from tannery effluent using fabricated sulfated carboxymethyl cellulose NF[29]. However, with emerging software and technology AI and ML comes into domain in modern engineering practices. All these latter technologies are very much superior to the former ones in terms of efficiency and computational time and good output predictions. The latter technologies several tools are present like ANN, Supported Vector Machines (SVM), Regression Tress (RT) and many more. All these tools are used for specific purpose and as per requirements of work[30]. In a work by researchers uses ANN for daily engineering applications solutions and that generated model was used and that model provides justified answer[31].

Stefano *et al.* generated a successful regression tree-based model which successfully predicted potential milk production which were affected by types of plants, soil and management factors[32].

AI and ML tools works using function of 'black box' principles, which eliminates the need for extensive system knowledge. When some traditional techniques are used to generalize trend and prediction of parameters, they take much time and resources. Compared to that sufficient set of experimental data given as an input, enables the AI tools to predict the trend with accuracy and precision for unseen data also. ANN modelling at very first state depends upon architecture or topology and modelling parameter. Some of the most common used ANN topography are Multilayer Perceptron (MLP), Radial Basis Function Neural Network (RBFNN), Recurrent Neural Network (RNN), Elman Neural Network (ENN), and Deep Neural Network (DNN). MLP is the most common in use and has the ability to deal with complex problems[33].

An ANN with an MLP configuration consists of at least three layers: an input layer, a hidden layer, and an output layer. Additionally, a hidden layer can have one or more hidden layers; all of these layers are connected to one another in a linear or non-linear manner depending on the input data. The input layer is the first layer that receives input data, which can be fed either vertically or horizontally. The hidden layer is the second layer that is deployed to process the data. The output layer is the last layer that provides us with the result that is generated for the hidden layer. An important information for ANN data processing is data flow direction. There is two different data flow direction: feed-forward and feed-backward.

i. Feed-forward flow direction is where the Data is moving as a signal in one direction and not returning back, giving output.

ii. Feed-backward flow direction is a flow where generated output is again feedback as an input to any previous layer, forming a loop and making it more complex.

For simplicity, we are using feed-forward direction. Respective layer has a fixed number of neurons in it; the number of neurons in the input layer is determined by the input responses provided during initial stage, and the number of neurons in the output layer is determined by the desired number of predictions. On the other hand, the number of neurons in the hidden layer can be altered to suit the needs and type of processing, ranging from one to as many as feasible. A precise balance is needed since, as increase the number of neurons in the hidden layer, calculation time will likewise grow.

Fig. 2 is 3:9:1 MLP-ANN configuration, where input layer have 3 neurons, hidden layer have 9 neurons additionally 1 bias and output layer have 1 neurons. Every neuron has two set of task to perform as shown in Fig. 3. First task is called the Summing Junction task described as S in Fig. 3, where all the output data from previous layer is fed as input ranging from X_i to X_n with an assigned weight W_i to W_n, respectively. Weight of an input value signifies importance for the process. To that additionally a constant value called bias b is added for normalizing the summing junction value and this make a proper summing junction output. Eq. 1 is the summing junction equation.

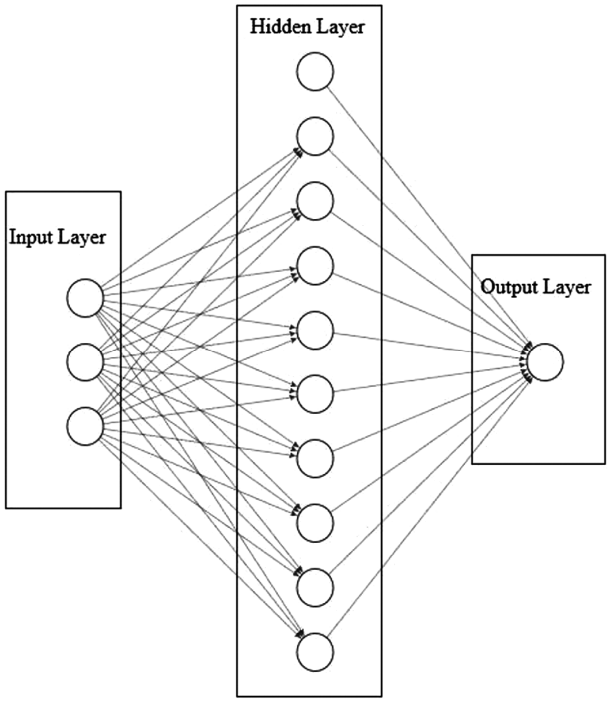

Fig. 2 — Feed Forward MLP-ANN architecture

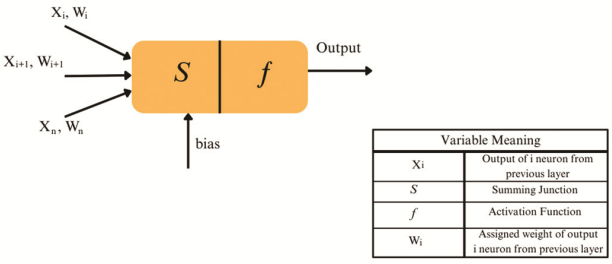

Fig. 3 — Working of Neuron

$$S = \sum_{m=1}^{n_{(j-1)}} \left(a_{m(j-1)} w_{m(j-1)}\right) + b_j \quad \ldots (1)$$

Where S is summing junction, $a_{m(j-1)}$ and $w_{m(j-1)}$ are the output value and associated weight from previous layer respectively. $n_{(j-1)}$ is the number of neurons in $(j-1)$ layer and b_j is bias value and j is the current layer.

The second task for neuron working is feeding these summing junction output data to the activation function described as f, which the user will select when the ANN is configured. There are three most common activation functions, and they are stated in Table 1 with their equations. For this study we will be considering pure linear activation function as it has a range of working from [-∞, ∞]. So, the need for normalization is eliminated.

Modelling of an ANN is done in three levels: training, validation, and test. The data gets divided into unequal sets, where maximum of feed data is used for training, around 70% and rest 30% is used for validation and test. This 30% can be used equally or unequally.

During the training phase, two types of training are done. The first is supervised training. Where training of the ANN is done in such a way that input responses are provided with the corresponding desire output or target values. This is done for the network to adjust itself with the expected output. By altering its weight, bias value, or by changing the number of iterations, also known as epochs. The second is unsupervised training where no target values are provided. Network is allowed to train by itself because this training takes a lot of time as well as all the alterations in weight and bias value are to be done manually. We chose supervised training.

To evaluate the performance of ANN loss functions are used, and there are several loss functions. Some of the common ones are Mean Square Error (MSE), Root Mean Square Error (RMSE), and Sum of Squared Error (SSE). MSE is the most commonly used. Eq. 2 shows MSE mathematical formula.

$$MSE = \frac{1}{n}\sum_{i=1}^{n}(y_{exp} - y_{model})^2 \quad \ldots (2)$$

In Eq. 2, n is the number of total samples, y_{exp} is experimental output and y_{model} is model output (which are predicted). Therefore, for simplicity, MSE is the average square difference between output and target. Achieving a minimum loss function while maintaining a precise relationship between responses and the target value can be accomplished by making several adjustments to the trained network. The term for this procedure is ANN training process. These training of ANN is done by and suitable ANN training algorithm. Table 2 shows various Training Algorithms with their Syntax. For our study we will consider all three algorithms and compare them with each other, the best one will be selected for simulation study. In this study, we have chosen a feed-forward back propagation network with a single hidden layer. To check the accuracy, MSE is deployed as a loss function.

Table 1 — Activation Function with their equation

Activation function	Equation
Logistic sigmoid	$f(x) = \frac{1}{1+e^{-x}}$
Hyperbolic tangent sigmoid	$f(x) = \frac{e^{2x}-1}{e^{2x}+1}$
Pure linear	$f(x) = x$

Table 2 — Different types of Training Algorithms corresponding their MATLAB Syntax

Training Algorithm	MATLAB Syntax
Levenberg-Marquardt algorithm	trainlm
Bayesian regulation	trainbr
Scaled Conjugate Gradient	trainscg

Results and Discussion

ANN modelling and simulations

ANN is supported by a number of open-access libraries, including Python, Chainer, Swift AI, and others. However, the ANN modelling in our study is done using MATLAB (version R2014a). In MATLAB typing the command "nnstart" into the command window, window will display and this is GUI (guided user interface) for neural networks is this new window. Neural Net Fitting, Neural Net Pattern Recognition, Neural Net Clustering, and Neural Net Time Series are the four new applications that have a path from this GUI. The neural net fitting method is selected to create the regression model. However, the Neural Net Fitting interface can also be accessed directly by using the command "nftool" in the command box.

Neural Net Fitting GUI opens in a new window. We need to initially submit the target and input data. The data is then compared with the GUI to see if it is

presented in increasing rows or increasing columns. Should the uploaded data be in ascending columns and we have selected a row format, a warning indicating that the uploaded data does not match will appear at the bottom. You can get rid of that caution by selecting the right format. The next button is chosen once the data has matched.

On selecting next, a new interface appears in which the total number of data is divided into three different sets for training, validation, and test. By default, 70% of the data is used for training, 15% of data is used for validation, and the remaining 15% of data is used for test; however, all this percentage can be changed by selecting the icon next to the percentage. In this study, we provide 60 sets of data as input. Five input parameters were given: TMP, feed concentration, temperature, feed flowrate and time pH value for entire study is kept constant. In the present work, all the experimental data sets have been taken from earlier work[28] and in that study all experiments were performed at the same pH Accordingly Modelling and simulations have been done using the base data. For the target value, we give the % of the rejection value. Therefore, for training, 42 data sets were used, for validation, 9 data sets were used, and for test another 9 data sets were used. All the input parameters and their respective ranges are provided in Table 3.

By making an appropriate adjustment, we click on the next button. A new interface appears in which we have to select the number of neurons/ nodes as per requirement. 10 neurons in the hidden layer are selected for this respective study. After selecting the number of neurons, we select the next button. A new window appears. In that window, we will select the training algorithm for our study. We have chosen all 3 algorithms, as already discussed, and the results are shown in Table 4, where all 3 algorithms' Coefficients of Correlation (R) are shown.

From analyzing the graph it is observed that Bayesian Regulation algorithm is the best among all as R value is best i.e., 1. So for this study Bayesian regulation algorithm is considered for simulation. All plots of regression curve from respective trained algorithm are shown in Fig. 4.

Four regression plots generated, i.e., training, validation, and test, and the last one is a combination of all data sets and makes it one graph. The first three graphs, which are training, validation and test, use their respective dataset, which we have given in the initial stage. In all graphs, X-

Table 3 — Input parameter with their ranges

Input Parameter	Operating Range
Operation time (min)	0-20
Feed Ph	8
Temperature (K)	293-303
Concentration of Feed (mg/L)	10-50
Flowrate of Feed (L/min)	9-17
Transmembrane Pressure (bar)	2.95-8.47

Table 4 — R-value obtained by various training algorithms used in the study

Name of algorithms	Training (R)	Validation (R)	Testing (R)	All (R)
Levenberg-Marquardt	0.99977	0.99894	0.99704	0.99898
Bayesian regulation	1	-	0.99999	1
Scaled Conjugate Gradient	0.99104	0.99572	0.98462	0.99056

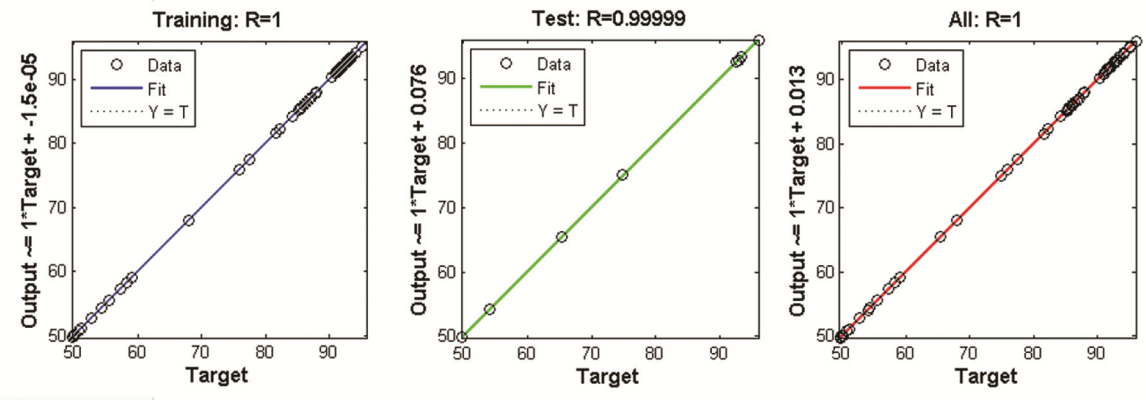

Fig. 4 — Regression curves from ANN study

axis represents the target value and Y-axis represents the output that the ANN generated after taking a close look at the graphs. We observe 'o' points which represents the actual point of target and corresponding output. Second is dotted line '-----Y=T' which represents the ideal scenario. The third and last one which is continuous line is Fit line which is making an ideal fit using all the 'o' points and this fit line then generates an R-value by comparing itself with the ideal scenario i.e. '-----Y=T'. Next is performance graph as depicted in Fig. 5.

Performance plot is generated between epochs and the chosen loss function, i.e., MSE, where again there are three coloured lines and a dotted line. These 3 coloured lines, blue, green, and red, represent three sets of data, i.e., training, validation, and test, respectively. The fourth dotted line is the best line, which is parallel to X and Y-axis and tell the attained MSE and corresponding epochs. To check model performance, training and validation losses are checked at a particular value, where higher losses on both categories indicate that the trained model is under-fit and if training loss is low but validation losses is still high, it indicates that the trained model is over-fit. Optimal fitting is achieved when both training and validation losses are less. The analysis of graphs suggests that at the 100th epoch, MSE is least i.e., 4.7862×10^{-7}.

Fig. 6 is the error histogram. This histogram is between errors and instances, where error is the difference between targets and output. In histogram, X-axis represents errors and Y-axis represents instances. This plot provides us with wholesome knowledge about error for all phases, i.e., training, validations, and test. The fourth line, which is yellow line is also generated, signifies 'zero error' and means that at that point, the target value and output value are the same and the error generated is zero or approaching zero for every instance.

However, if a better solution is not achieved in the first iteration, we can also retrain ANN again by clicking retrain, and when having the best train ANN, click on the next button. Then, a new window will appear and simulate option is present in that window. By clicking that option, we can input a set of data and simulate it. For simplicity, we input all the responses to the trained model to predict the data. These predicted values are plotted along with the target values, as shown in Fig. 7. Here, the X-axis shows the instances or sample number, which was

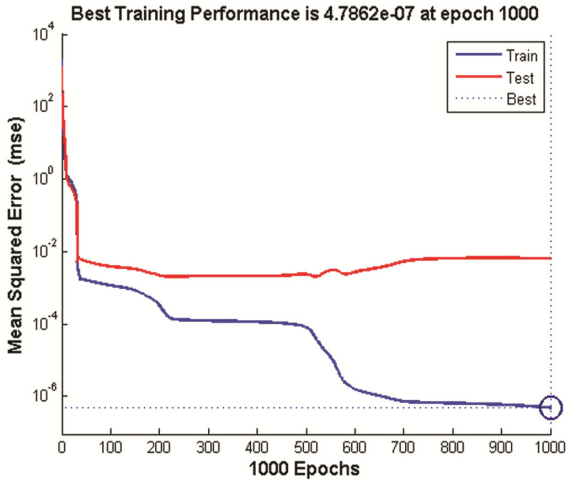

Fig. 5 — Performance plot from ANN study

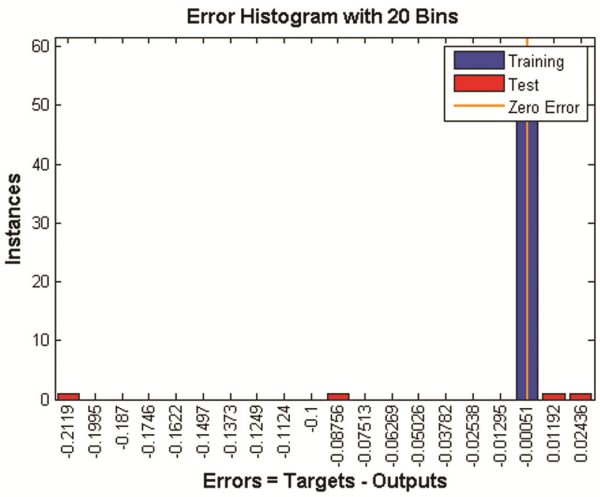

Fig. 6 — Error histogram generated from ANN study

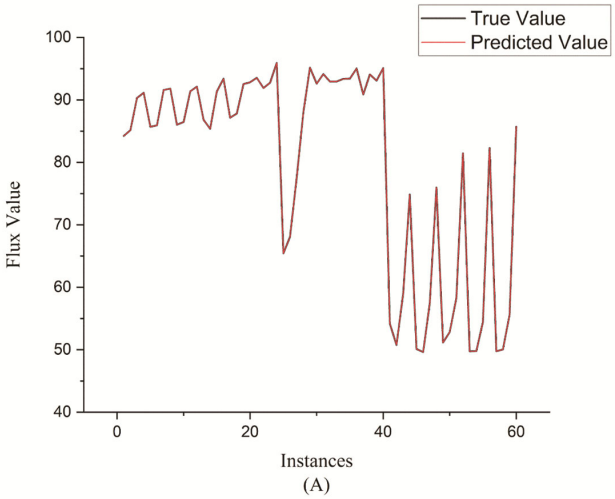

Fig. 7 — Plot on Instances vs various Output

60 data sets in total, and the Y-axis shows the output. Here, two sets of data are plotted: data 1 is target data or experimentally attained data, which is black in colour, and Data 2 is predicted data from trained ANN, which is red in colour. From analysis, it is observed that both values are mostly similar and coincide.

Fig. 8 plots the error between both data for better understanding. The X-axis is the instances or sample number, which was 60, as discussed above, and the Y-axis is the error, ranging from 0.1 to -0.1. From analyzing the plot, it is observed that the error is very little, mostly zero. This also accounts for better training justification. Now, the effect of various operating parameters and how they influence % rejection will be analyzed.

Effect of increasing Feed Flowrate and Feed Concentration on %Rejection

Fig. 9 is an isometric projection of Feed Concentration vs Feed Flowrate where output measured is the %Rejection when TMP, Temperature and pH are kept constant i.e. 7.09 bar, 303 K and 8, respectively. From analysis, it is observed that when Feed Concentration is high, %Rejection is very high irrespective of any Feed Flowrate. This particular notion happens as the inlet feed concentration increase more and more molecules of As(III) start to accumulate on membrane feed site making a hindrance for permeation for any further As(III) molecule and that is the reason for increase in %Rejection. That similar trend happens when concentration decreases %Rejection decreases[34]. However, in prima facie, considering Feed Flowrate,

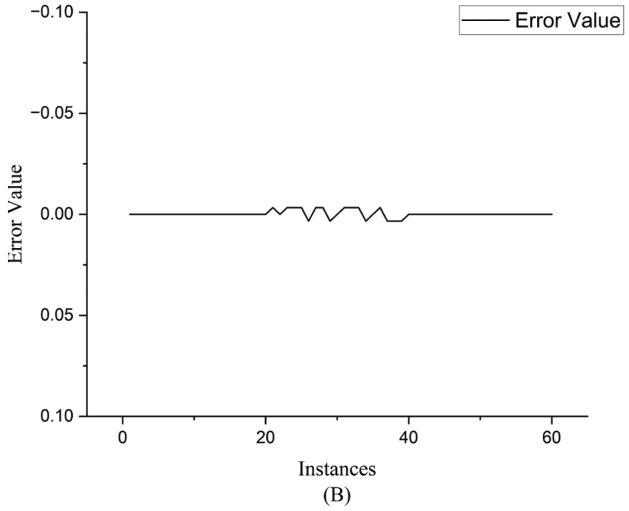

Fig. 8 — Plot on Instances vs error value

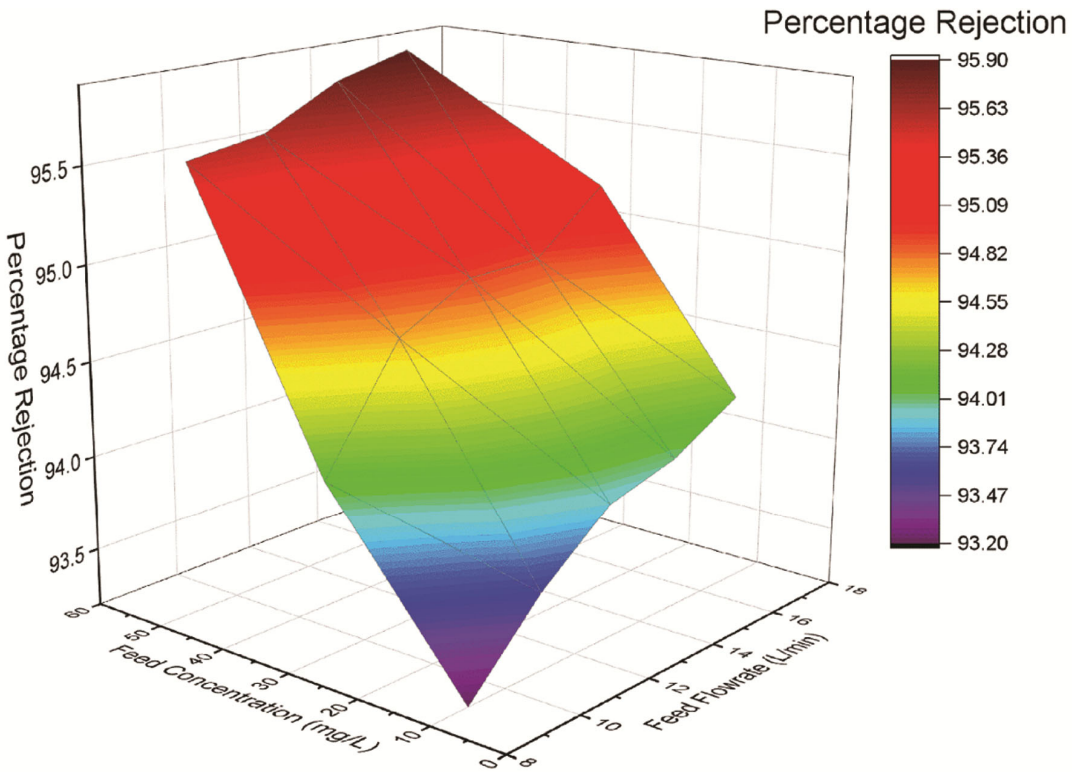

Fig. 9 — Isometric plot on effect of Feed Flowrate, Feed Concentration on %Rejection

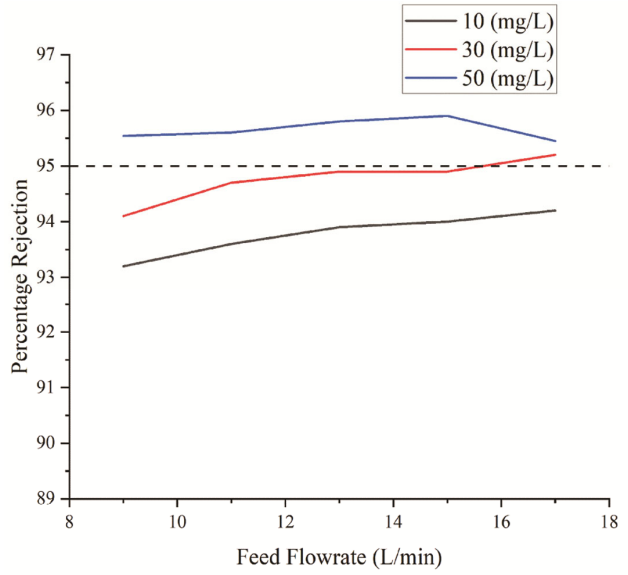

Fig. 10 — plot between Feed Flowrate vs %Rejection with varying Feed Concentration

it is observed that when the Flowrate increase %Rejection also increases at constant concentration of feed. The reason of this observation is that rate of accumulation of As(III) molecule on the permeate site is increased and that make %Rejection increased as making a resistance to flow[35]. However, % Rejection gradually decreases when Feed Concentration and Feed Flowrate decreases. Although irrespective of any Feed Concertation and Flow rate, %Rejection is above 90%.

For better understanding, Fig. 10 is analyzed, where X-axis is Feed Flowrate and Y-axis is %Rejection and %Rejection is measured with increasing Feed Flowrate at different Feed Concentrations. From observations, value of %Rejection is not changing much from 93.2% when Feed Flowrate and Feed Concentration is 9 L/min and 10 mg/L, respectively, to 95.6% when Feed Flowrate is 15 L/min and Feed Concentration is 50 mg/L, which is very less. However, if we consider a benchmark for %Rejection at 95, which is represented by (- - - -) line, it is observe that stream with Feed Concentration 50 mg/L is always above the benchmark %Rejection at any Feed Flowrate. This is because of the maximum number of As(III) molecules will be present on non-permeate side at this values and they will also acting as a further resistance for flow as discussed in previous paragraph and observed in past work [reason 1]. However, when Feed Flowrate increases beyond 15 L/min, there is a slight decrease in %Rejection and that is due to membrane fouling and this fouling make increase in pore size which will allow As(III) molecules to permeate more into the permeate stream is observed during past research work[28]. However, when Feed Flowrate is high i.e. beyond 16 L/min, the stream with Feed Concentration 30 mg/L also crosses benchmark %Rejection. When the flowrate is at 12.5 L/min stream with Concentration 30mg/L is very much close to benchmark value because here the rate of accumulation of undesired molecules i.e. As(III) is slow so it crosses the benchmark %Rejection late [reason 2]. So, for long duration of working stream with 30 to 50 mg/L is most suitable with 12.5 to 17 L/min.

Effect of Increasing Feed Concentration and TMP on %Rejection

Fig. 11 is the isometric projection of Feed Concentration vs TMP where output to be found is %Rejection and keeping Feed Flowrate, pH and Temperature Constant i.e. 12.5L/min, 8 and 303, respectively. It is observed that with increase in TMP and having constant Feed Concentration, the value of % Rejection increases. The reason for this is that NF is PDM which means that the driving force for NF to work is applied pressure difference so as the more the pressure difference more the %Rejection and Separation of undesired substance [reason 3]. However, when TMP value crosses 6 bar value, the %Rejection decreases and that can be seen. That happens because the NF membrane doesn't hold such a high pressure and such a high pressure will make wear and tear of membrane and pore size will be altered [reason 4]. On contrast to that if, we increase Feed Concentration and keep the TMP constant then %Rejection increases to a maximum value approaching 97% rejection.

For better understanding considering Fig. 12 where X-axis is Feed Concentration, Y-axis is %Rejection and five different coloured line represents TMP lines. From analyzing, it is observed that on increasing concentration, %Rejection also increases irrespective of any TMP. This is due to effect of steric hindrance effect[36]. As on increasing Feed Concentration there might be a possibility of adsorption of As(III) on membrane pores and that will decrease the pore size making more difficult to permeate from membrane. However, if Feed Concentration is kept constant and TMP is changed then we observe that on increase in pressure until 7.09 bar, %Rejection increases. This is due to fact of dilution effect where on increasing

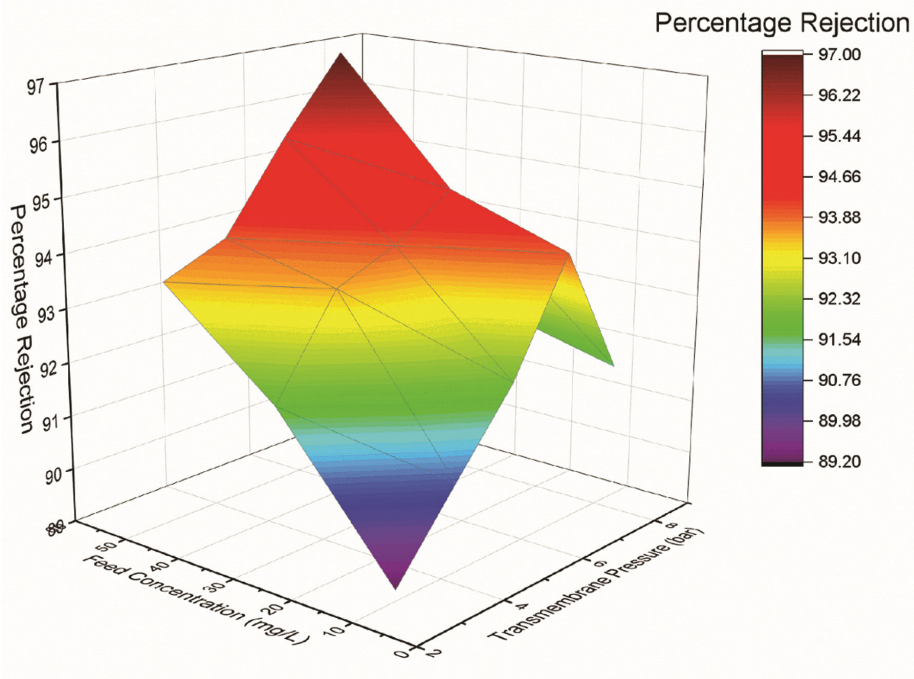

Fig. 11 — Isometric plot on effect of TMP, Feed Concentration on %Rejection

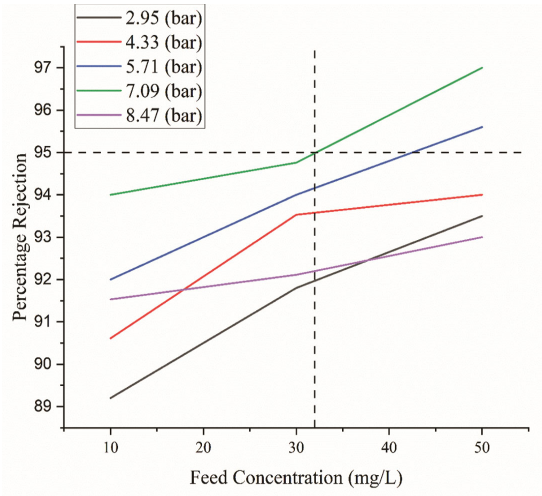

Fig. 12 — Plot between Feed Concentration vs % Rejection with varying TMP

pressure leads more solvent on permeate side. Then from 7.09 to 8.47 bar, % rejection decreases this is due to swelling of pores which does allows for easy permeate path for As and that is also observed by researchers[37]. However if a benchmark value of %Rejection value is consider at 95, it is observed that stream with TMP 7.09 bar reaches and crossed benchmark %Rejection with Feed Concentration above 30 mg/L. Then after second stream to be considered is 5.71 bar and to corresponding concentration is high of about 45 mg/L. These results suggest that for better %Rejection, optimum working conditions would be when TMP, Feed Flow rate and Feed concentration would be in between 5.71 to 7.09 bar, 12.5 to 17 L/min and 30 to 50 mg/L respectively.

Conclusion

This study successfully employed an artificial neural network to model the NF membrane for rejection of As(III). MSE was chosen as loss function to evaluate modelled ANN and least value of MSE i.e. 4.7862 $\times 10^{-7}$ was found when in hidden layer there were 10 number of neurons with a correlation coefficient of 1 during training, test and validation phases. Afterwards, effects of input parameters like Feed Concentration, TMP and Feed Flow rate were also gauged for an optimized value of %Rejection. Maximum %Rejection was received when Feed Concentration was in between 30 to 50 mg/L irrespective of TMP. The maximum value of TMP obtained when pressure was in range from 5.71 to 7.09 bar and if we increase pressure, %Rejection decreases as compared to the optimum range. However, for any Feed Flow rate value of %Rejection received was mostly above 90%. However, if Feed concentration were 30 mg/L then operating Feed Flow rate would be above 12.5 L/min and when operated with 50 mg/L Feed concentration flow rate should be in between 9 to 17 mg/L.

References

1 Department of Water Resources, River Development & Ganga Rejuvenation, Ministry of Jal Shakti, Govt of India.
2 Preventing disease through healthy environments, WHO (2022).
3 Shankar S, Shanker U & Shikha, Arsenic contamination of groundwater: A review of sources, prevalence, health risks, and strategies for mitigation, *Sci World J*, 2014 (2014) 304524.
4 Berg M, Tran H C, Nguyen T C, Pham H V, Schertenleib R & Giger W, As contamination of groundwater and drinking water in Vietnam: A human health threat, *Environ Sci Technol*, 35 (2001) 1.
5 Cheryan M, Ultrafiltration & Microfiltration Handbook, (1998).
6 Selvi K, Pattabhi S & Kadirvelu K, Removal of Cr(VI) from aqueous solution by adsorption onto activated carbon, *Bioresour Technol*, 80 (2001) 87.
7 Kongsricharoern N & Polprasert C, Electrochemical precipitation of chromium (Cr^{6+}) from an electroplating wastewater, *Water Sci Technol*, 31 (1995) 109.
8 Shen F, Chen X, Gao P & Chen G, Electrochemical removal of fluoride ions from industrial wastewater, *Chem Eng Sci*, 58 (2003) 987.
9 El-Hefny N E, Comparison of liquid-liquid extraction of Cr(VI) from acidic and Alkaline solutions by two different amine extractants, *Sep Purif Technol*, 67 (2009) 44.
10 Nguyen V T, Vigneswaran S, Ngo H H, Shon H K & Kandasamy J, As removal by a membrane hybrid filtration system, *Desalination*, 236 (2009) 363.
11 Kozlowski C A & Walkowiak W, Removal of chromium(VI) from aqueous solutions by polymer inclusion membranes, *Water Res*, 36 (2002) 4870.
12 Atia A A, Synthesis of a quaternary amine anion exchange resin and study its adsorption behaviour for chromate oxyanions, *J Hazard Mater*, 137 (2006) 1049.
13 Rajendran R M, Garg S & Bajpai S, Study of transport models for as removal using nanofiltration process: Recent perspectives, *Emerg Technol Environ Bioremed*, (2020) 391.
14 Santafé-Moros A, Gozálvez-Zafrilla J M & Lora-García J, Experimental simulation of continuous nanofiltration processes by means of a single module in batch mode, *Sep Purif Technol*, 187 (2017) 233.
15 Fang J & Deng B, Rejection and modeling of arsenate by nanofiltration: Contributions of convection, diffusion and electromigration to as transport, *J Memb Sci*, 453 (2014) 42.
16 Criscuoli A & Figoli A, Pressure-driven and thermally-driven membrane operations for the treatment of as-contaminated waters: A comparison, *J Hazard Mater*, 370 (2019) 147.
17 Ribera G, Llenas L, Martínez X, Rovira M & de Pablo J, Comparison of nanofiltration membranes performance in flat sheet and spiral wound configurations: A scale-up study, *Desal Water Treat*, 51 (2013) 458.
18 Ku Y, Chen S W & Wang W Y, Effect of solution composition on the removal of copper ions by nanofiltration, *Sep Purif Technol*, 43 (2005) 135.
19 Saitúa H, Campderrós M, Cerutti S & Padilla A P, |Effect of operating conditions in removal of as from water by nanofiltration membrane, *Desalination*, 172 (2005) 173.
20 Hu K & Dickson J M, Nanofiltration membrane performance on fluoride removal from water, *J Memb Sci*, 279 (2006) 529.
21 Mittal S, Gupta A, Srivastava S & Jain M, Artificial neural network based modeling of the vacuum membrane distillation process: Effects of operating parameters on membrane fouling, *Chem Eng Process Process Intensif*, 164 (2021) 108403.
22 Jawad J, Hawari A H & Javaid Z S, Artificial neural network modeling of wastewater treatment and desalination using membrane processes: A review, *Chem Eng J*, 419 (2021) 129540.
23 Bowen W R, Jones M G, Welfoot J S & Yousef H N S, Predicting salt rejections at nanofiltration membranes using artificial neural networks, *Desalination*, 129 (2000) 147.
24 Zhao Y, Taylor J S & Chellam S, Predicting RO/NF water quality by modified solution diffusion model and artificial neural networks, *J Memb Sci*, 263 (2005) 38.
25 Shetty G R & Chellam S, Predicting membrane fouling during municipal drinking water nanofiltration using artificial neural networks, *J Memb Sci*, 217 (2003) 69.
26 Darwish N A, Hilal N, Al-Zoubi H & Mohammad A W, Neural networks simulation of the filtraton of sodium chloride and magnesium chloride solutions using nanofiltration membranes, *Chem Eng Res Des*, 85 (2007) 417.
27 Arya R K, Sharma J, Shrivastava R, Thapliyal D & Verros G D, Modelling of surfactant-enhanced drying of poly(styrene)-p-xylene polymeric coatings using machine learning technique, *Coatings*, 11 (2021) 1529.
28 Rajendran R M, Garg S & Bajpai S, Modelling of as (III) removal from aqueous solution using film theory combined spiegler-kedem model: Pilot-scale study, *Environ Sci Pollut Res*, 28 (2021) 13886.
29 Gasemloo S, Khosravi M, Sohrabi M R, Dastmalchi S & Gharbani P, Response surface methodology (RSM) modeling to improve removal of Cr(VI) ions from tannery wastewater using sulfated carboxymethyl cellulose nanofilter, *J Clean Prod*, 208 (2019) 736.
30 Shetty G R, Malki H & Chellam S, Predicting contaminant removal during municipal drinking water nanofiltration using artificial neural networks, *J Memb Sci*, 212 (2003) 1.
31 Alanis A Y, Arana-Daniel N & López-Franco C, Artificial neural networks for engineering applications, (2019).
32 Stefano D C, Lando G, Malegori C, Oliveri P & Sammartano S, Prediction of water solubility and setschenow coefficients by tree-based regression strategies, *J Mol Liq*, 282 (2019) 401.
33 Iqbal J, Tyagi A & Jain M, Artificial neural network based modelling of liquid membranes for separation of dysprosium, *J Rare Earths*, 41 (2023) 440.
34 Pérez-Sicairos S, Lin S W, Félix-Navarro R M & Espinoza-Gómez H, Rejection of As(III) and As(V) from as contaminated water via electro-cross-flow negatively charged nanofiltration membrane system, *Desalination*, 249 (2009) 458.
35 Al-Rashdi B A M, Johnson D J & Hilal N, Removal of heavy metal ions by nanofiltration, *Desalination*, 315 (2013) 2.
36 Dash B & Kumar A, Nanofiltration for textile dye-water treatment: Experimental and parameter estimation studies using a spiral wound module and validation of the spiegler-kedem-based model, *Sep Sci Technol*, 52 (2017) 1216.
37 Dziubek J, As removal from industrial wastewater, In Proceedings of the E3S Web of Conferences, 17 (2017).